A Robust Statistical Framework for Instantaneous Electroencephalogram Phase and Frequency Estimation and Analysis

Reza Sameni, Esmaeil Seraj

A Robust Statistical Framework for Instantaneous Electroencephalogram Phase and Frequency Estimation and Analysis

Reza Sameni* and Esmaeil Seraj

School of Electrical and Computer Engineering, Shiraz University, Shiraz, Iran.
Tel: +98 71 3613 3169, Fax: +98 71 3647 3367, E-mail: rsameni@shirazu.ac.ir, e.seraj@cse.shirazu.ac.ir

Abstract

Background: The instantaneous phase (IP) and instantaneous frequency (IF) of the electroencephalogram (EEG) are considered as notable complements for the EEG spectrum. The calculation of these parameters commonly includes narrow-band filtering followed by the calculation of the signal's analytical form. The calculation of IP and IF is highly susceptible to the filtering parameters and background noise level, especially in low analytical signal amplitudes.
New Method: Herein, a Monte Carlo estimation scheme is proposed for robust estimation of the EEG IP and IF. It is proposed that any EEG phase-related inference should be reported as an average with confidence intervals obtained by repeating the IP and IF estimation under infinitesimal variations (selected by an expert), in the algorithmic parameters such as the filter's bandwidth, center frequency and background noise level. In the second part of the paper, a stochastic model consisting of the superposition of narrow-band foreground and background EEG is used to derive probability density functions of the instantaneous envelope (IE) and IP of EEG signals, which justify the proposed Monte Carlo scheme.
Results: It is rigorously shown that the IP/IF estimation quality highly depends on the IE and any phase/frequency interpretations in low IE are statistically unreliable and require a hypothesis test.
Comparison with Existing Methods: The impact of the proposed method on previous studies, including time-domain phase synchrony, phase resetting, phase locking value and phase amplitude coupling are studied with examples.
Conclusion: The findings of this research can set forth new standards for EEG phase/frequency estimation and analysis.

Keywords: Electroencephalogram phase calculation; time-domain phase synchrony; phase resetting; phase locking value; phase amplitude coupling; phase slipping

1. Introduction

In recent decades, the instantaneous phase and frequency of the electroencephalogram (EEG) have received great attention in neuroscience and brain research communities, as a notable complement for the EEG spectral contents. The concept has found broad applications in *brain computer interface* (BCI) systems [1, 2], cognitive studies [3, 4] and brain connectivity assessment [5, 6]. Phase-related quantities have also been widely used in the analysis of clinical and pathological cerebral conditions, including epilepsy [7, 8], dementia [9, 10], autism [11] and many more. Recent studies have also sought the relationship between the EEG phase and *event-related synchronization* (ERS) and *de-synchronization* (ERD) [12, 13].

The reliable estimation of the EEG phase and frequency is an essential prerequisite for all these studies. Various techniques such as the Hilbert transform (HT), wavelet transform (WT), and other time/frequency representations have been utilized for reliable and unambiguous phase calculation (cf. Section 2). Among all, the HT has been considered the most reliable means of EEG phase estimation, as a method which does not violate the physical and theoretical conditions essential for instantaneous phase extraction [14]. However, a major difficulty in using the HT (and other instantaneous EEG phase extraction methods) is to distinguish between physiological state transitions due to brain activity and spurious variations, spikes and phase jumps— known as "phase slipping" [15]. It has been previously reported that unambiguous measurements of the EEG phase cannot be made around phase slipping epochs, nor near the ends of signal segments [15, 16]. Some minimum required signal-to-noise levels have also been empirically found for detecting oscillatory neural activities in presence of background noise [17].

Other aspects of EEG phase extraction and analysis, such as temporal properties and band-pass filtering requirements have been investigated in [15, 18]. The authors reported notable discontinuities (phase slipping events) in the EEG phase calculated from the human scalp and attempted to minimize these effects. A comprehensive study was performed on various phase extraction tools (particularly HT and WT) and their impacts and interpretations in neural synchrony [19]. In [14], physical and theoretical conditions and steps required for obtaining a meaningful phase sequence were extensively studied, besides investigating the most reliable approaches for this purpose. In a recent study [20], the impact of narrow-band filtering was studied in true versus spurious phase synchronization using synthetic data models.

Manuscript under review, April 2017

Although the problem of reliable EEG phase and frequency estimation has been extensively studied in the neuroscience and brain communities, due to the lack of a stochastic framework, the results and discussions regarding the so-called phase slipping phenomenon remain qualitative and descriptive— commonly stated as a note of caution— instead of providing precise guidelines for the extraction and interpretation of the EEG phase/frequency and discriminating between true versus spurious phase jumps.

The objective of the current study is to propose a Monte Carlo estimation procedure for robust instantaneous EEG phase and frequency estimation using "minor" perturbations in the input signal and phase/frequency estimation algorithm parameters. The proposed method is very generic and does not rely on prior models for the EEG and the parameter perturbation order can be set by the expert depending on application.

In the second part of the paper, we adopt a model-based approach to justify the proposed Monte Carlo estimation procedure in a rigorous statistical framework. Using the most widely accepted EEG data model and profound theories from signal detection and estimation [21, 22, 23, 16], it is shown that issues such as EEG phase slipping and phase/frequency deviations are unavoidable (yet predictable), and spurious phase variations can be probabilistically discriminated from physiologically relevant EEG phase/frequency variations. The EEG signal's instantaneous analytical form envelope, which has been empirically used in previous studies, is shown to have a fundamental impact on the accuracy of the EEG phase contents.

From an application viewpoint, the authors have recently shown the applicability of the hereby presented method for BCI [24] and sleep stage scoring [25] applications.

In Section 2, the basic steps required for EEG phase extraction are reviewed and the motivation of the current study is shown using a synthetic data example. The proposed Monte Carlo phase/frequency estimation method is detailed in Sections 3-4. This method is statistically justified and used for deriving statistical properties of narrow-band EEG in background noise in Section 5. The practical implications of the proposed method are detailed in Section 6. Various applications of the proposed framework and its impact on previous EEG phase studies are presented in Section 7.

2. Instantaneous Envelope, Phase and Frequency Calculation

The classical procedure of calculating the instantaneous envelope (IE), instantaneous phase (IP) and instantaneous frequency (IF) of a signal is to use its analytical form [23]. These measures are only uniquely defined for narrow-band signals. Therefore, considering a discrete-time signal y_n (such as an EEG), it is first bandpass (BP) filtered around the desired center frequency $\omega_0 = 2\pi f_0/f_s$ with a narrow bandwidth *bw*.

$$x_n = \mathcal{BP}(y_n; p) = y_n * h_n \tag{1}$$

where h_n is the equivalent BP filter's impulse response, $*$ denotes convolution, f_s is the sampling frequency in Hz, and

$$p = \{type, method, \omega_0, bw, \delta_s, \delta_p, \cdots\} \tag{2}$$

is the set of design parameters describing the BP filter, including the filter *type*, design *method*, center frequency ω_0, bandwidth *bw*, stop-band attenuation δ_s, pass-band ripple δ_p, etc. The parameter set p plays a major role in the current study. A detailed discussion is presented in Section 3.1, regarding the parameter set selection.

Next, the *analytical form* of the BP filtered signal is calculated using the discrete-time Hilbert transform $\mathcal{H}\{\cdot\}$.

$$\tilde{x}_n = x_n + j\mathcal{H}\{x_n\} \tag{3}$$

The IE, IP, and IF are calculated from the analytical form as follows.

$$\mathrm{A}_n \triangleq \sqrt{\mathcal{R}e(\tilde{x}_n)^2 + \mathcal{I}m(\tilde{x}_n)^2} \tag{4}$$

$$\phi_n \triangleq \mathrm{atan2}[\mathcal{I}m(\tilde{x}_n), \mathcal{R}e(\tilde{x}_n)] \tag{5}$$

$$f_n \triangleq \frac{f_s}{2\pi}[\phi_n - \phi_{n-1}] \mod 2\pi \tag{6}$$

where atan2 represents the four-quadrant inverse tangent and the difference operator in (6) is used as an approximation for phase differentiation (cf. [22] for alternative approximations). In order to avoid instantaneous jumps in the IF, the IP sequence is commonly *unwrapped* before calculating the difference in (6).

The upper mentioned stages of IE, IP, and IF calculation (BP filtering plus analytical signal calculation) are the main stages of the majority of EEG phase analysis studies. This procedure is fully deterministic and does not account for the stochastic properties of the EEG.

In order to show the motivation of the current study, let us consider a synthetic signal diluted by narrow-band additive noise, as shown in Fig. 1. The signal model is as follows:

$$y(t) = A(t)\cos(2\pi \int_0^t f(\tau)d\tau) + n(t) \tag{7}$$

where $A(t) = \sin(2\pi \times 3.1t) + 0.7\sin(2\pi \times 2.7t + \pi/6)$ is a slowly varying amplitude, $f(t) = \sin(2\pi \times 0.8t) + 20$ Hz is the instantaneous frequency and $n(t)$ is narrow-band Gaussian noise centered around $f_0 = 20$ Hz and a variance adjusted to set the total *signal-to-noise ratio* (SNR) of $y(t)$ to 25 dB. We consider two cases for the effective bandwidth of $n(t)$: 2 Hz and 2.01 Hz, obtained by filtering two ensembles of white noise using bandpass filters with the same center frequency f_0 and 0.01 Hz of difference in their effective bandwidths. The data is sampled at $f_s = 125$ Hz for illustration. According to Fig. 1, it is clearly seen that although the amplitude variations are rather slow and the initial phase of $y(t)$ is constant, abrupt random phase jumps and instantaneous frequency errors are inevitable in low analytical signal envelopes. In these cases, the difference between the two filters becomes significant. This difference can be numerically explained by considering that in low signal amplitudes, the argument of atan2 in (5) is singular, as it fluctuates around *zero-divided-by-zero* and a small difference in the filtering scheme or background noise can cause large phase variations (even beyond $\pm\pi$) and randomize the IF, as shown in the last row in Fig.

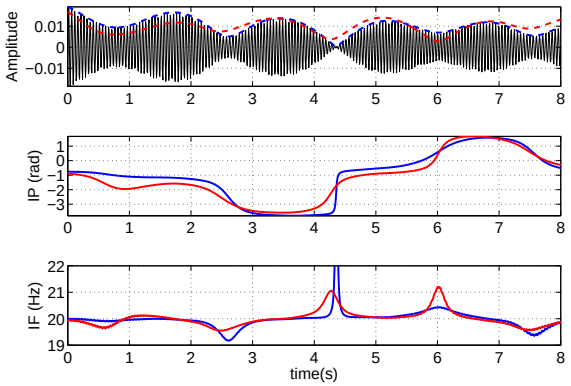

(a)

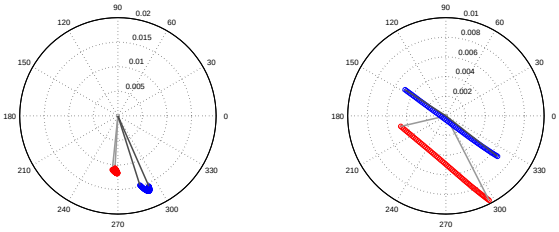

(b) (c)

Figure 1: (Top row) a synthetic signal and its analytical form envelope in dashed line using the two filtering schemes detailed in Section 2; (second row) the instantaneous phase in both cases; (third row) the estimated instantaneous frequency and the true instantaneous frequency in dashed lines; (last row left) the polar representation of a 0.5 s segment of the analytical form around t = 3.5 s with a high envelope; (last row right) the polar representation of a 0.5 s segment of the analytical form around t = 4.3 s with a low envelope. Notice the angle between the first and last sample of the 0.5 s segments in both cases.

1. This suggests that the probability of phase jumps and the variance of the IF, somehow increase in low analytical signal envelopes.

This example shows the necessity of a statistical framework for the problem of EEG IP and IF analysis, which systematically considers the effect of low/high instantaneous envelope and background noise and is robust to minor variations in filtering parameters and the phase extraction algorithm.

3. Method: Robust EEG Phase/Frequency Estimation

Following the explanations and the example in Section 2, it is noticed that EEG phase and frequency features can be highly susceptible to background noise and minor variations in the extraction algorithm (e.g. the bandpass filtering procedure), especially during epochs of low analytical signal envelopes. To overcome this limitation, we propose that due to the stochastic nature of the EEG, the estimated phase and frequency features should be studied under minor variations in non-physiological aspects of phase extraction, including: EEG measurement quantization noise and infinitesimal variations in the filtering parameters. Our basic assumption throughout this work is that:

A1. *For any significant EEG-based physiological inference, there exists a range of measurement and algorithmic parameter variations (defined by an expert), which can be considered to be irrelevant to the undergoing physiological phenomenon.*

In other words, we assume that physiologically significant EEG characteristics (spectral, phase, frequency, etc.) are robust to *infinitesimal perturbations* in: 1) the signal's amplitude, and 2) the phase extraction method (e.g. the bandpass filter's design parameter set). This assumption is indeed intuitive and the definition of *infinitesimal perturbations* is subjective and highly dependent on the undergoing physiological activity (brain task). Nevertheless, we assume that for any physiological experiment, the expert can set a bound on the algorithm parameters, beyond which any parameter variations are irrelevant to the underlying experiment.

Assumption (A1) is supported by the fact that the sub-frequency bands defined in the EEG phase analysis literature are highly subjective and minor deviations in the center frequencies, bandwidths, and even filter design technique are implicitly assumed to be irrelevant to the phase study. To the best of the authors' knowledge, despite the rich literature on EEG phase, only some general guidelines have been proposed for the phase extraction procedure [15, 26], and researchers have been basically using arbitrary and un-unified narrow-band filtering and phase extraction schemes in their studies.

Another source of measurement variability, which is commonly neglected in practice, is due to quantization and background noise. Therefore, if the input signal is *dithered* by minor additive noise, at the order of the background EEG level or at the quantization level of the analog-to-digital convertors (ADC) used for digitizing the EEG, the foreground EEG is again expected to remain consistent under such minor dithers.

Based on these assumptions we propose that:

P1. *The procedure of EEG phase and frequency estimation should consist of a Monte Carlo sweep over random perturbations of measurement and algorithm parameters (background noise level, filter's bandwidth, center frequency, etc.) at a user-defined level. The estimated EEG parameters should be reported with their mean and confidence intervals over this Monte Carlo simulation.*

This procedure is rather general and it can be implemented in different forms. For a given EEG signal y_n, Algorithm 1 is hereby proposed as a realization of proposition (P1), to find robust values and statistical confidence intervals for IP and IF estimates.

For illustration, Fig. 2 shows 30 s of a typical EEG, recorded in a BCI experiment; together with its IE, IF and unwrapped IP, calculated using Algorithm 1 for $N = 50$ iterations. The sampling frequency of the signal is $f_s = 160$ Hz. For better visualization of the phase fluctuations, in Fig. 2, the unwrapped phase has been subtracted by $2\pi(f_0/f_s)n$, which is the instantaneous phase of a sinusoidal oscillator with a fixed initial phase. The BP filter is a zero-phase forward-backward filter obtained from an order six moving average lowpass filter prototype, shown in Fig. 3. The center frequency of the filter is $f_0 = 13.1$ Hz

Algorithm 1 Robust Instantaneous EEG Phase and Frequency Estimation

Require: A filter design parameter set p as defined in (2).

Define: An *algorithmic variation irrelevancy bound* (AVIB), including the background noise level ($\delta\lambda$) and filter design parameter variation range (δp). Note: The algorithm reduces to the conventional deterministic phase estimation technique by setting $\delta\lambda = 0$ and $\delta p = 0$.

1: **for all** $k = 1, \cdots, N$ **do**

2: Design a bandpass filter with perturbed design parameter set $p^{(k)} = p + \delta\rho^{(k)}$, where the parameter perturbations are $\delta\rho^{(k)} \leq \delta p$.

3: Add minor noise to the input EEG at an order of $\delta\lambda$, to obtain dithered randomized ensembles of the EEG:

$$d_n^{(k)} = y_n + \nu_n^{(k)} \tag{8}$$

We assume $\nu_n^{(k)} \sim \mathcal{N}(0, \epsilon_n^2)$ to be Gaussian noise and the dither variance $\epsilon_n^2 \leq \delta\lambda$.

4: Filter $d_n^{(k)}$ using bandpass filters designed with the perturbed design parameter set $p^{(k)}$:

$$x_n^{(k)} = \mathcal{BP}(d_n^{(k)}; p^{(k)}) \tag{9}$$

5: Calculate the analytical form of the filtered ensemble:

$$\tilde{x}_n^{(k)} = x_n^{(k)} + j\mathcal{H}\{x_n^{(k)}\} \tag{10}$$

6: Calculate the IE, IP, and IF:

$$X_n^{(k)} = |\tilde{x}_n^{(k)}| \tag{11}$$

$$\theta_n^{(k)} = \text{atan2}[\mathcal{I}m(\tilde{x}_n^{(k)}), \mathcal{R}e(\tilde{x}_n^{(k)})] \tag{12}$$

$$f_n^{(k)} = \frac{f_s}{2\pi}[\theta_n^{(k)} - \theta_{n-1}^{(k)}] \mod 2\pi \tag{13}$$

7: **end for**

8: Find the ensemble averages and variances of the parameters

$$\bar{x}_n = E\{\tilde{x}_n^{(k)}\}, \quad \lambda_n^x = E\{(\tilde{x}_n^{(k)} - \bar{x}_n)^2\} \tag{14}$$

$$\bar{X}_n = E\{X_n^{(k)}\}, \quad \lambda_n^X = E\{(X_n^{(k)} - \bar{X}_n)^2\} \tag{15}$$

$$\bar{\theta}_n = E\{\theta_n^{(k)}\}, \quad \lambda_n^\theta = E\{(\theta_n^{(k)} - \bar{\theta}_n)^2\} \tag{16}$$

$$\bar{f_n} = E\{f_n^{(k)}\}, \quad \lambda_n^f = E\{(f_n^{(k)} - \bar{f_n})^2\} \tag{17}$$

where $E\{\cdot\}$ represents the sample mean over the N generated ensembles[1].

9: Calculate the confidence intervals of the estimated parameters: $\sigma_n^X = \sqrt{\lambda_n^X}$, $\sigma_n^\theta = \sqrt{\lambda_n^\theta}$, and $\sigma_n^f = \sqrt{\lambda_n^f}$.

(the peak of the power spectral density as shown in Fig. 4) and the effective bandwidth is 1 Hz. In each of the N trials, this filter has been perturbed with random deviations of the bandwidth ranging from zero to 0.05 Hz, the center frequency f_0 has been perturbed with a uniform random value in the range of $f_0 \pm 10^{-2}$ Hz, and the dither $\nu_n^{(k)}$ in each iteration is a zero-mean Gaussian random variable with a standard deviation $\epsilon_n = 0.1$, which is smaller than the quantization level of the 14-bit ADC used for sampling the EEG signal. The gray shades in Fig. 2, show the results of N trials overlaid. The average instantaneous frequency $\bar{f_n}$ and the confidence intervals bounded by $\bar{f_n} \pm \sigma_n^f$ are also shown. The frequency response of the N perturbed bandpass filters are shown in Fig. 3. It is seen that although the algorithmic and noise level variations are negligible from the physiological viewpoint, the IP and IF results are significantly different, especially during the low analytical signal segments of the EEG.

3.1. Parameter Selection

The proposed framework is generic and its parameters should be selected for each application. Various aspects of the parameter selection are discussed in what follows.

3.1.1. Filter Design Scheme

The BP filter is a linear transform. Accordingly, the phase of x_n over the entire Nyquist band, is the summation of the input signal's phase and the filter's phase. Therefore, for phase-based studies, linear-phase finite impulse response (FIR) are commonly used, which preserve the input signal phase difference and do not add any phase distortions; in contrast to infinite impulse response (IIR) filters, which are nonlinear phase. However, the order of narrow-band FIR filters can become very high, resulting in long transient response effects. Moreover, the addition of even a linear phase to the input signal can cause fake phase jumps due to the phase wrapping of the filter's phase. To avoid this, we herein use zero-phase forward-backward filtering (FIR or IIR) [2], which does not cause any phase distortions and guarantees the phase synchrony between the input and output of the BP filter. This procedure is evidently non-causal, which is not a limitation for offline phase analysis.

3.1.2. Filter Design Parameter Set

The BP filter specifications such as the center frequency, bandwidth, and design method are all subjective and may be selected according to physiological ground truth (as considered in all previous studies). According to Assumption 1, for each application, the parameter deviations considered during the Monte Carlo simulation are selected such that the deviated filter specifications would be physiologically "irrelevant" for the application of interest. For example, consider an EEG with a dominant 7-12 Hz (alpha-band) spectral density. Physiologically, many experts would consider a 0.1 Hz of filter bandwidth deviation to be irrelevant for such an experiments (at least according to

[2] Zero-phase forward-backward filtering can be implemented using the *filtfilt* function in Matlab, Octave, or R.

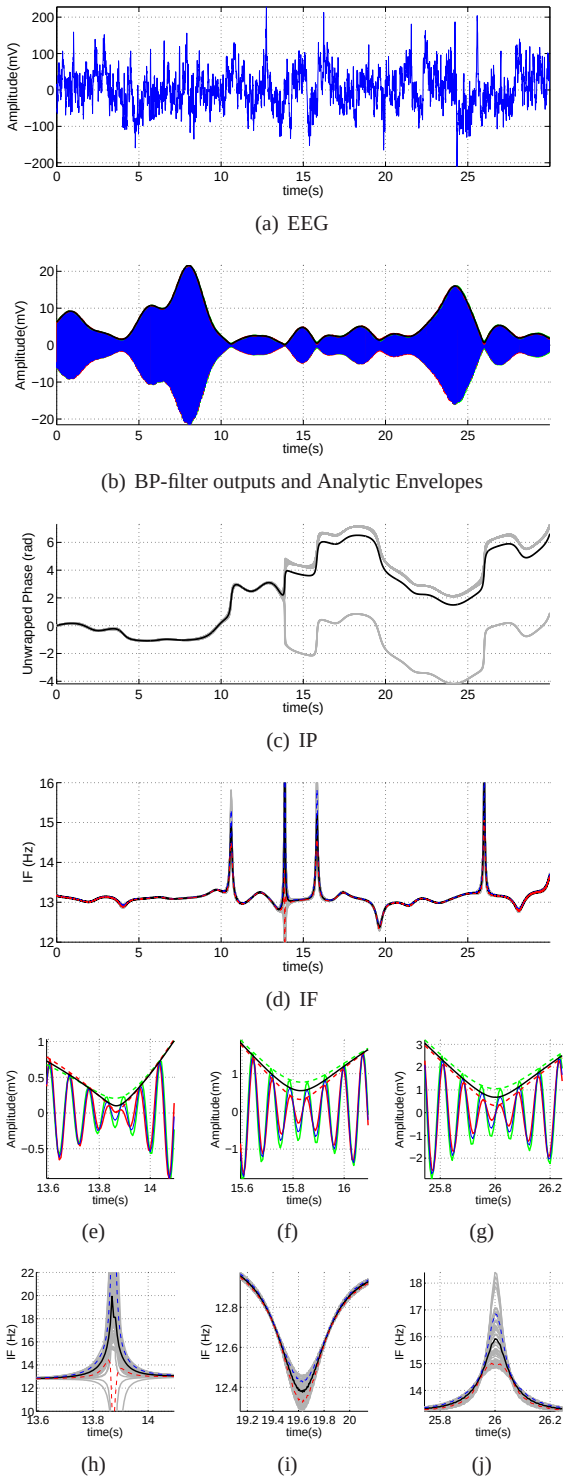

Figure 2: (a) A sample EEG segment; (b) the bandpass filtered signals using three BP filters with f_0 = 13.09, 13.1, 13.11 Hz and the corresponding analytical signal envelopes; (c) the unwrapped IP of fifty perturbed ensembles with their highlighted mean; (d) the IF of fifty perturbed ensembles with f_n, and $\overline{f_n} \pm \sigma_n^f$ confidence intervals; (e)-(g) a zoom-in of three IE segments where the black, red and green traces correspond with the output of BP filters centered at f_0, $f_0 - \delta f$ and $f_0 + \delta f$, respectively, and envelopes shown in thick black, dashed red and dashed green; (h)-(j) zoom-in of three IF segments. Notice the random $\pm\pi$ phase jumps around t = 13.9 s, which coincide with a notch in the IE.

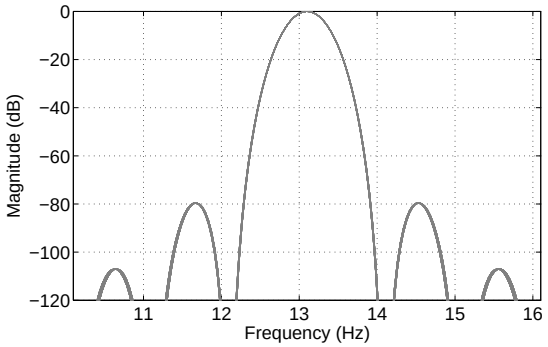

Figure 3: The overlaid magnitude response of $N = 50$ order six moving average filters obtained by perturbing the design parameters, used for the results in Fig. 2. The difference between the filter responses are assumed to be irrelevant for EEG phase analysis. Refer to Section 3 for further details.

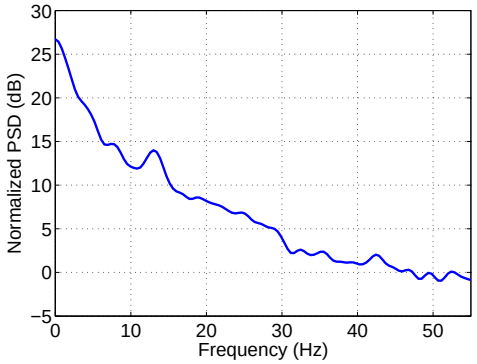

Figure 4: Normalized power spectral density (PSD) of the sample EEG segment of Fig. 2

the current literature). Therefore, randomization of the BP filter bandwidth at this level will help the identification of reliable and unreliable EEG parameters.

Depending on the filter design scheme, the filter's parameter variations can be done in various domains. For instance, one may prefer to perform the perturbation in the zero-pole configuration of a predefined filter (as recently proposed in [24]). In this case, the filter should be checked for stability after the random pole perturbations and the poles should be preserved inside the unit circle. Moreover the conjugate symmetry of the zeros and poles need to be preserved, in order to guarantee the realness of the filter coefficients.

3.1.3. Dither Level

The dither level should be at the same order (or smaller than) the expected background noise. The quantization noise of the analog to digital convertors used in EEG sampling is an inevitable source of background noise, which can be simply found by studying the electronic specifications of the ADC used in the EEG measurement system. The background EEG is another source of background noise. However, the background EEG is rather subjective and model dependent and may be subject to a debate among experts.

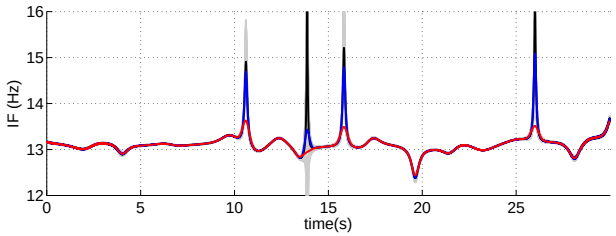

Figure 5: The estimated IF of 50 ensembles overlaid (gray shades); the average IF (black); the KF-smoothed IF with $\gamma_n = 10^{-3}$ (blue) and $\gamma_n = 10^{-5}$ (red).

4. Post-Processing: Temporal Filtering of Instantaneous EEG Parameters

The ensemble averaging technique proposed in Stage 8 of Algorithm (1) does not consider the temporal correlations of the IE, IP, or IF. By assuming a temporal dynamic model for these parameters, the estimation quality may be further improved by conventional filtering and smoothing schemes such as the Kalman filter or Particle filter (also known as Sequential Monte Carlo). Herein, for proof of concept, we assume a first order auto-regressive dynamic model for the IP and apply a classical Kalman filter to improve the IP and IF estimates.

$$\begin{aligned} \theta_n &= \theta_{n-1} + w_n \\ \phi_n &= \theta_n + \psi_n \end{aligned} \tag{18}$$

where $w_n \sim \mathcal{N}(0, \gamma_n^2)$ is considered as process noise, and $\psi_n \sim \mathcal{N}(0, \sigma_n^2)$ is the observation noise. For this model, it can be shown that the Kalman filter equations have a single tunable parameter σ_n^2/γ_n^2, which can be adjusted proportional to the phase and frequency variances obtained in (16) and (17). In Fig. 5, the IF of the sample EEG segment from Fig. 2 is shown after applying the Kalman smoother for $\sigma_n^2 = \lambda_n^f$ (as defined in (17), and two values $\gamma_n = 10^{-3}$ and $\gamma_n = 10^{-5}$. Apparently, the results are smoother for smaller values of γ_n (the filter relies on the first-order dynamics) and become closer to the observed noisy IF for larger values of γ_n. This example is only shown as proof of concept. The rich literature on Kalman filtering and its extensions can be used in future studies for robust IP and IF estimation, using suitable temporal priors.

5. A Theoretical Model-Based Justification; Statistical Properties of Narrow-Band EEG

The empirical method and results presented in Section 3, demonstrate the susceptibility of EEG phase and frequency estimates in low analytical signal amplitudes. However, for a formal description of these findings, a data model is required. Herein, we use the most widely accepted model in the literature [27, 28, 29], to extract statistical properties of narrow-band EEG. Although, the hereby developed formulations are in accordance with empirical results on real data, the statistical framework proposed in this section is subject to debate, depending on the acceptance or rejection of the model for specific applications (as with all model-based techniques).

5.1. Data Model

An implicit assumption in most EEG phase analysis studies is that a desired (narrow-band) brain activity, referred to as *foreground EEG* in the sequel, coexists in a pool of *background EEG*, considered as noise. The background EEG is considered to be spontaneous (as compared with the foreground EEG). It is the superposition of numerous simultaneous and non-coherent cortical activities, which according to the *central limit theorem* tends to a Gaussian distribution and is spread over the entire frequency band of study. On the other hand, the foreground EEG can be the result of some mental activity, external stimuli (audio, visual, etc.), or any other evoked activity, which discriminates it from the spontaneous EEG. Based on these assumptions, the following additive model can be considered as a generic model for the EEG signal at the BP filter output.

$$x_n = X_n \cos(\omega_0 n + \theta_n) + v_n = s_n + v_n \tag{19}$$

where the first part (s_n) models the foreground EEG, X_n is the non-negative foreground envelope with slow variations (low-pass with respect to the center frequency ω_0), θ_n is the instantaneous foreground EEG phase (again with rather slow variations), and v_n is the narrow-band counterpart of the background EEG, which generally overlaps with the foreground EEG spectrum. Due to the linearity of the BP filter, the background EEG remains Gaussian through the filtering process, i.e., $v_n \sim \mathcal{N}(0, \sigma_n^2)$.

In this model, the rather slow variations of X_n and θ_n (approximately constant over very small temporal windows) is the main assumption that discriminates the foreground and background EEGs. The objective of EEG phase analysis is to estimate the phase signal θ_n.

If the BP filter is sufficiently narrow-band (as required for a canonical definition of the IE, IP, and IF [21, 23]), its analytical form can be written as follows.

$$\tilde{x}_n = x_n + j\mathcal{H}\{x_n\} = X_n e^{j(\omega_0 n + \theta_n)} + \eta_n = A_n e^{j(\omega_0 n + \phi_n)} \tag{20}$$

where $\eta_n = r_n e^{j(\omega_0 n + \psi_n)}$ ($r_n \geq 0$) is the analytical form of v_n—a complex valued Gaussian random process with zero-mean independent real and imaginary parts and σ_n^2 variance [30, Ch. 8]. The phasor diagram of the foreground plus background EEG is shown in Fig. 6 for illustration.

This additive model is perhaps the most generic model for narrow-band EEG and in accordance with the most widely accepted data models in EEG phase analysis studies (cf. [27] for a detailed discussion about the most common EEG phase models). Previous studies have mainly studied the narrow-band foreground part of model (19) within a deterministic framework; neglecting the statistical properties of the background EEG. The basic idea that is followed in this work is that the problem should be studied in a stochastic framework and the signal detectability and reliability of the desired EEG phase totally depend on the instantaneous envelopes and variances of the foreground and background EEG.

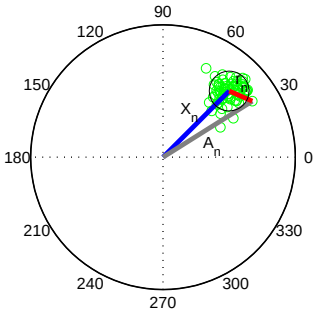

Figure 6: The phasor diagram of seventy-five data points (green) of foreground plus background EEG. The black solid circle has a radius of $2\sigma_n$. Assuming a Gaussian distribution for the background EEG, 68% of the points fall within this circle.

5.2. *Probability Density Functions of the EEG envelope and phase*

The statistical properties of the signal model in (19) have been extensively studied in the signal processing literature [31, 30]. Herein, we use some of these well-known properties to find a statistically justifiable (reliable) method for EEG phase analysis. For simplicity, we assume the sine wave envelope X_n and the noise variance σ_n^2 to be known (or estimated as discussed in Section 5.4).

5.2.1. *pdf of narrow-band background EEG*

Considering a Gaussian probability density function (pdf) for the background EEG, the magnitude and phase of its analytical form ($\eta_n = r_n e^{j(\omega_0 n+\psi_n)}$) are independent [30]. In absence of a foreground activity ($X_n = 0$), the background EEG magnitude has a Rayleigh distribution and the phase is uniform over $[-\pi, \pi]$:

$$f(r_n|\sigma_n^2) = \begin{cases} \dfrac{r_n}{\sigma_n^2}\exp\left(-\dfrac{r_n^2}{2\sigma_n^2}\right), \text{for } r_n \geq 0 \\ 0, \text{elsewhere} \end{cases} \tag{21}$$

$$f(\psi_n|\sigma_n^2) = \begin{cases} \dfrac{1}{2\pi}, \text{for } -\pi \leq \psi_n \leq \pi \\ 0, \text{elsewhere} \end{cases} \tag{22}$$

5.2.2. *pdf of narrow-band foreground plus background EEG*

In presence of foreground EEG, due to the Gaussian assumption on the background EEG, it can be shown that the envelope and phase of the analytical form (20) have the following joint pdf:

$$f(A_n, \phi_n, \theta_n|X_n, \sigma_n^2) = f(A_n, \Delta\phi_n|X_n, \sigma_n^2) = \frac{A_n}{2\pi\sigma_n^2}\exp\left(-\frac{A_n^2 + X_n^2 - 2X_nA_n\cos(\Delta\phi_n)}{2\sigma_n^2}\right) \tag{23}$$

where $\Delta\phi_n = \phi_n - \theta_n$ is the instantaneous random phase difference (error) between the noisy and noiseless sinusoidal part of the model (the observed versus foreground EEG phases in our case).

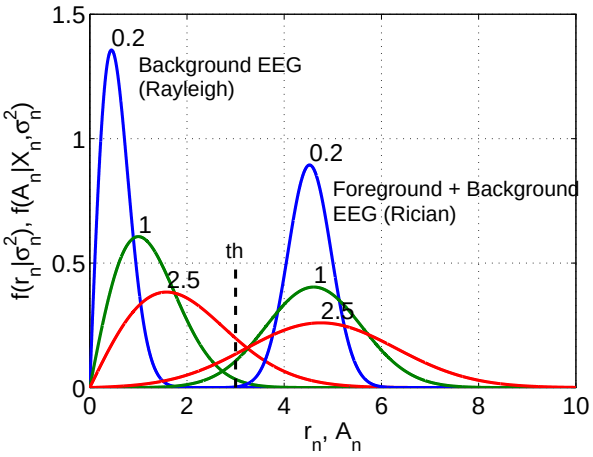

Figure 7: Envelope distributions of Gaussian background EEG (left three curves) and foreground EEG oscillations plus Gaussian background EEG (left right curves) for $X_n = 4.5$ and $\sigma_n^2 = 0.2$, 1, 2.5, equivalent to $\text{SNR}_n = 17$, 10, 6 dB.

In this case, the envelope and phase are no longer independent (a key point in our study). The marginal distribution of the analytical envelope has a Rician distribution.

$$f(A_n|X_n, \sigma_n^2) = \frac{A_n}{\sigma_n^2}\exp\left(-\frac{A_n^2 + X_n^2}{2\sigma_n^2}\right)I_0\left(\frac{X_nA_n}{\sigma_n^2}\right) \tag{24}$$

where $I_0(\cdot)$ is the *modified Bessel function of the first kind* [30, Ch. 8]. Using the Bayes' rule and combining (23) and (24), the conditional pdf of the phase error $\Delta\phi_n$ is found.

$$f(\Delta\phi_n|A_n, X_n, \sigma_n^2) = f(\Delta\phi_n|\kappa_n) = \frac{\exp(\kappa_n\cos(\Delta\phi_n))}{2\pi I_0(\kappa_n)} \tag{25}$$

where $\kappa_n \triangleq A_nX_n/\sigma_n^2$. Apparently, this distribution is symmetric ($E\{\Delta\phi_n|A_n, X_n, \sigma_n^2\} = 0$) and $E\{\Delta\phi_n^2|A_n, X_n, \sigma_n^2\}$ is an envelope-dependent phase-error variance. These properties support the assumptions required for the Kalman smoothing stage described in Section 4.

Finally, integrating (23) over A_n, the marginal distribution of the IP error is found.

$$f(\Delta\phi_n|X_n, \sigma_n^2) = f(\Delta\phi_n|\rho_n) = \frac{1}{2\pi}\exp(-\rho_n^2)[1+ \sqrt{\pi}\rho_n\cos(\Delta\phi_n)\,\text{erfcx}\,(-\rho_n\cos(\Delta\phi_n))] \tag{26}$$

where $\rho_n \triangleq \sqrt{\text{SNR}_n} = X_n/\sqrt{2\sigma_n^2}$ denotes the root square of the instantaneous SNR and erfcx$(\cdot)$ is the *scaled complementary error function*.

The envelope, phase error, and conditional phase error distributions of narrow-band Gaussian background EEG and foreground plus background EEG are shown in Figs. 7, 8, and 9, respectively.

The calculation of the IF pdf additionally requires the joint pdf of θ_n and θ_{n-1}. Due to the lack of ground truth regarding the temporal dependence of the EEG phase, previous results on the IF pdf of sinusoidal signal plus noise [31, 32, 33], which either

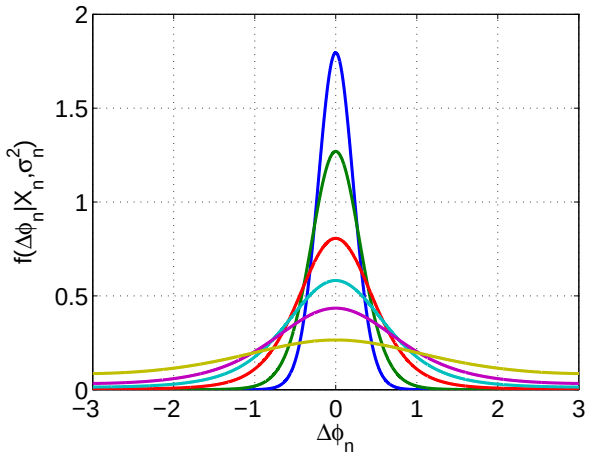

Figure 8: Phase distributions of foreground EEG oscillations plus Gaussian background EEG for $X_n = 4.5$ and from top to bottom $\sigma_n^2 = 1$, 2, 5, 10, 20, and 100, equivalent to $\text{SNR}_n = 10$, 7, 3, 0, -3, and -10 dB.

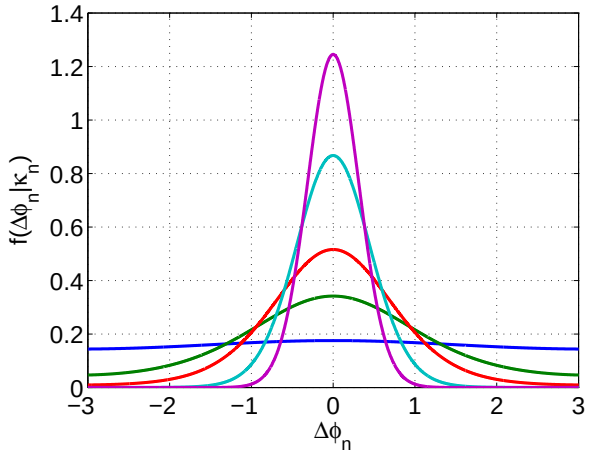

Figure 9: Conditional phase error distributions of foreground EEG oscillations plus Gaussian background EEG for $\kappa_n = 10$, 5, 2, 1, 0.1 (from top to bottom).

assume a constant or fully random phase are not directly applicable in this case. A rigorous approach is to model the temporal dynamics of the IP, e.g., by assuming a Markov model for the IP, which is beyond the scope of the current study. However, as a rule of thumb, previous research have shown that the IF pdf becomes sharper around ω_0 as the IP becomes more correlated in time (has slow temporal variations) [32]. Moreover, the IF pdf is peaked around ω_0 in high SNR and it tends to a uniform distribution over $[-\pi, \pi]$ (the entire Nyquist band) in low SNR.

These pdfs have also been used to extract lower bounds on the estimation variance of the IP and IF using different assumptions on the temporal structure of the IP [34, 35]. Again, as a general rule of thumb, the Cramér-Rao lower bound (CRLB) of the IP error variance is commonly inversely proportional to the SNR [36].

In summery, all the probability density functions derived in this section depend on the background EEG variance and the instantaneous analytical signal envelope of the foreground EEG. Specifically, in low analytical signal envelopes, the probability of phase error tends to a uniform distribution over $[-\pi, \pi]$, which is in accordance with the results previously shown in Fig. 2.

5.3. Signal Detectability

Regardless of the presence or absence of a foreground EEG activity, the procedure of IP calculation (narrow-band BP filtering, analytical signal calculation followed by IP estimation) always produces an output; even from pure random background EEG (noise). But how can one guarantee that there has been some foreground activity? Here, we either require physiological ground truth obtained from the experimental setup or other modalities (e.g., simultaneous MEG, fMRI, etc.), or complementary information from multiple EEG leads. In absence of reliable ground truth, one faces a statistical *hypothesis test*. At each time instant, there are two possible hypothesis:

$$\begin{aligned} H_0: &\quad x_n = v_n \\ &\quad \text{(background EEG alone)} \\ H_1: &\quad x_n = X_n \cos(\omega_0 n + \theta_n) + v_n \\ &\quad \text{(background plus foreground EEG)} \end{aligned} \tag{27}$$

The decision is apparently probabilistic. The objective is to determine the most likely hypothesis, which meets some predefined *probability of detection* (p_d) and *probability of false alarm* (p_f).

The detection of a sinusoidal in noise is a classical problem in detection theory [37, Ch. 6]. The hypothesis test is performed by setting an appropriate threshold *th* on the IE to meet the desired p_d and p_f. By definition and according to Fig. 7

$$\begin{aligned} p_f &= \int_{th}^{\infty} f(r_n|\sigma_n^2) dr_n \\ p_d &= \int_{th}^{\infty} f(A_n|X_n, \sigma_n^2) dA_n \end{aligned} \tag{28}$$

which depend on the instantaneous foreground and background EEG levels (the SNR). The curves for p_d as a function of the required SNR with p_f as parameter are shown in Fig. 10, for a fixed instantaneous phase $\theta_n = cte$. The same results are approximately applicable for sinusoids with slowly varying phase (as compared with the center frequency ω_0), a condition that is satisfied for narrow-band BP filtered EEG. Some useful rules can be derived from Fig. 10. For example, a 10 dB SNR is required to detect a foreground signal with a probability of 90% and p_f=1%. For the same p_f, the probability of detection drops below 10% in zeros or negative SNR. In practice, one may fix the desired p_d and p_f and find the corresponding SNR value from Fig. 10. By intersecting this value with the instantaneous SNR, one can determine the time instants for which the existence of foreground EEG activity are most (least) probable. These results are in accordance with the empirical SNR levels previously proposed for the detection of neural oscillations in background EEG [17].

The utilization of Fig. 10 requires the instantaneous SNR (or its estimate), which is not directly available for the EEG. A heuristic approach for estimating the EEG SNR is proposed in Section 5.4.

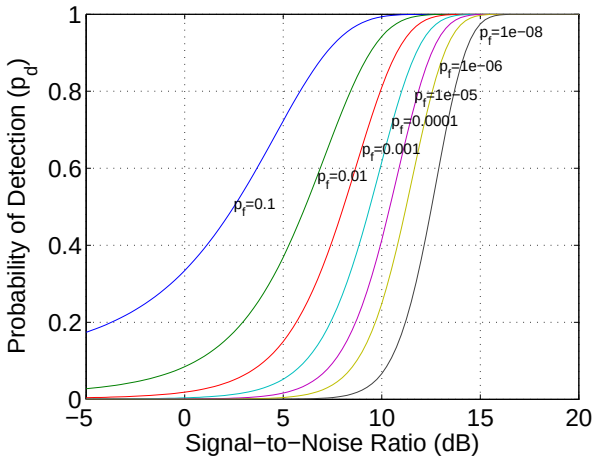

Figure 10: Detection probability (p_d) as a function of the required SNR with false alarm probability (p_f) as a parameter [37, Ch. 6]

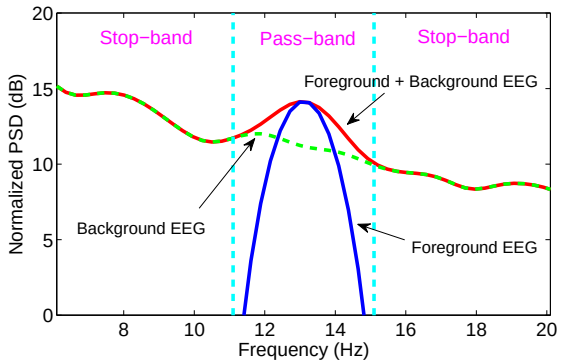

Figure 11: Normalized power spectral density (PSD) of a sample EEG segment and the estimated foreground and background EEG

5.4. Foreground/Background EEG SNR Estimation

The estimation of the instantaneous SNR requires some prior assumptions regrading the foreground and background EEG. Considering the additive data model proposed in Section 5.1, and considering the foreground EEG (s_n) and background EEG (v_n) to be uncorrelated, superposition holds between their power spectral densities (PSD):

$$S_x(f) = S_s(f) + S_v(f) \tag{29}$$

$S_x(f)$ can be directly estimated from the raw EEG. If we further assume that the background EEG is flat over the narrow-band filter's passband, the background EEG PSD $S_n(f)$ can be estimated from the neighborhood bands of the frequency band of interest as shown in Fig. 11, and $S_s(f)$ is found by subtracting $S_n(f)$ from $S_x(f)$. The area under these spectral estimates is equal to their total power. Therefore, the SNR in the filter's passband is obtained. The same method can be performed online, by estimating the PSD and SNR_n over a sliding window of the input signal (cf. [17] for a similar approach).

An alternative approach for SNR estimation is to use oscillatory signal tracking schemes (similar to the one developed in [38] for electrocardiogram denoising applications) to estimate the foreground EEG from x_n. Having an estimate of s_n, the background EEG and the instantaneous SNR can be found.

6. Interpretation of Instantaneous Envelope, Phase and Frequency Estimates

The results of previous sections has some major implications for a systematic interpretation of the EEG phase, including:

1. The confidence in signal detection, IP and IF estimations is directly related to the instantaneous SNR and envelope (X_n). In fact, considering a stationary background EEG variance ($\sigma_n = cte.$), in low foreground EEG envelopes (X_n), the accuracy of signal detection drops, the probability of phase slipping increases, and the IP/IF estimation qualities degrade. This suggests that IP and IF are only reliable in high SNR, and it is not possible to validate any phase or frequency activity without considering the instantaneous envelope of the analytical form of the EEG simultaneously.

2. The EEG IP and IF are stochastic parameters with SNR-dependent pdfs. As random variables, they can fluctuate within the range of their pdf. The confidence intervals of these parameters imply that as far as the estimated IP and IF are within the $\bar{\theta}_n \pm \sigma_n^{\theta}$ and $\bar{f}_n \pm \sigma_n^{f}$ ranges, the event is considered "normal". An odd event— having perhaps a physiological origin, such as phase resetting, etc.— may only be reported when the IP/IF exceed the normal range. This shows that phase/frequency jumps that occur in low analytical signal envelopes are statistically irrelevant and may not necessarily be associated to any biological origin. More rigorously, using the pdfs derived in Section 5.2, percentiles can be estimated for each of the estimated parameters to find the probability of a given IP or IF.

3. The randomized ensembles generated from the Monte Carlo scheme proposed in Section 3 can be considered as samples drawn from the density functions derived in Section 5.2. Considering the symmetry of the IP distribution, $\bar{\theta}_n$ yields the maximum a posteriori (MAP) estimate of the IP. For the IE (due to the right skew of its distribution) and IF (due to its possible pdf asymmetry, which depends on the temporal dynamics of the EEG phase), instead of taking the expectation of the randomized ensembles, the sample *mode* can be used to obtain the MAP estimate (which are no longer equal to $\bar{X}_n$ or $\bar{f}_n$).

4. Considering the fundamental role of the IE in phase analysis, a hypothesis that requires future studies is that many of the phase inferred parameters of the EEG, may in fact be associated to the analytical signal envelope, rather than the EEG phase. In other words, phase-related parameters such as phase resetting may be side effects of the signal's envelope drop, rather than being an independent physiological phenomenon.

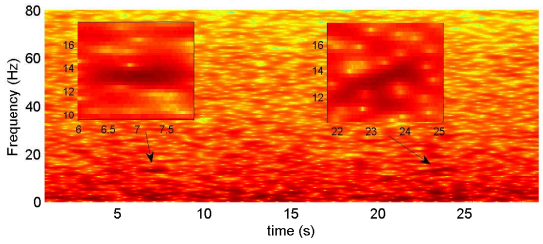

Figure 12: The short-time frequency transform (STFT) of a sample EEG. The left highlighted segment shows a vanishing component at a fixed IF; the right highlighted segment shows a component with varying IF, corresponding to scenarios (A) and (B) in Section 6.1, respectively.

6.1. Simultaneous Envelope, Phase and Frequency Variations

The implication of the previous study is that the instantaneous analytical signal envelope is highly fundamental for phase or frequency variations and phase and frequency measures become unreliable in low IE. However, further considerations are required for reliable interpretation of the IE. Consider the following scenarios, which both lead to a low analytical signal envelope:

A) Stationary IF (fixed phase shift) with a dropping IE

B) Stationary envelope with a varying IF (variable phase shift)

The two scenarios are shown in the short-time frequency transforms of a sample EEG segment in Fig. 12. In the first scenario, the IE is explicitly dropping; while in the second scenario, due to the variation of the IF, the signal is moving out of the narrow BP filter's pass-band, which indirectly results in an IE drop. In both cases, the estimated IP and IF become unreliable. However, only the first scenario can be considered as a statistical burden (without any physiological source); while the second scenario can frequently happen for an EEG to have minor fluctuations in the IF mode (considering the narrow-band of the BP filter), as in experiments with varying levels of consciousness or during sleep. In order to discriminate these scenarios, the analytical signal envelope can be tracked at the output of a filter bank with three filters: a BP filter centered at f_0 and two BP filters with minor center frequency deviations, centered at $f_0 - \delta f$ and $f_0 + \delta f$. In the first scenario the envelope at all three filter outputs will drop; while in the second scenario the envelope of the main BP filter (centered at f_0) will drop and the envelope of either the right or left vicinity frequency bands will increase. This simple frequency tracking scheme is a computationally efficient alternative for time-frequency analysis of the EEG.

Fig. 2(b) illustrates the idea. A sample EEG has been passed through three zero-phase BP filters with the same effective bandwidth 1 Hz, and center frequencies 13.09 Hz, 13.0 Hz, and 13.01 Hz ($\delta f = 0.01$ Hz). The resulting signals have been overlaid for comparison, with three highlighted segments shown in Figs. 2(e), 2(f) and 2(g). Due to the zero-phase (zero group-delay) property, the input and output of these filters are phase synchronous. Accordingly, Fig. 2(e) shows significant IE drops in all three BP filter outputs. Considering the IF of the same segment in Fig. 2(h) we notice the totally random behavior of the IF (positive and negative fluctuations around f_0), due to the very low IE of this segment. Fig. 2(f) shows another IE drop in all three BP filter outputs. Considering the IF in the same segment in Fig. 2(i) we notice that although the IF has a high variance in this segment, but all the randomized ensembles report an instantaneous frequency drop in this segment. The same phenomenon has occurred in Fig. 2(g) and Fig. 2(j); but this time with IF tendency towards frequencies above f_0.

7. Applications

The current study has significant implications in various EEG phase analysis applications. In this section, some of the major applications are studied with examples. In order to make the results reproducible, all source codes related to this study are online available in the *open-source electrophysiological toolbox* (OSET) [39][3].

7.1. Time Domain Synchrony and PLV

The synchronous firing of neurons within different brain regions has been considered as a potential source of EEG-level brain responses. Synchrony estimation consists of first calculating the phase sequences using electric or magnetic brain records and then quantifying the local stability of phase lock through computing the difference between these sequences [40]. In this context, phase-locking value (PLV) is one of the most common indexes used for calculating the coherency and synchrony between phase signals [40, 41]. The index is based on the phase difference (PD) between two EEG signals.

To show the importance of the proposed statistical approach in phase synchrony studies, the IP, IF and IE of five 20 s segments of simultaneous EEG channels are shown in Fig.13.

As illustrated in Fig.13, the initial observation shows a great synchrony between the IP of O1, P3, C3 and partially F3 (middle panel). Moreover, considering the FP1 as a reference signal, the inter-channel phase differences (PLVs), are showing a sort of *phase lock* or significant *phase shift* in the highlighted time epochs (indicated by boxes in Fig.13). Nevertheless, when comparing these plots with their corresponding IE (in the left panel of Fig.13), it is noticed that the spikes in the phase indexes are concurrent with low IE. Therefore, the phase effects are side-effects of a low analytical signal envelope during the same epochs. More specifically, the boxes indicated as (a) and (b) in the left panel have been selected such that the IE captured from electrode FP1 (the reference lead) includes two notches. During the same period, two big spikes can be observed in its corresponding phase derivatives in the middle panel of FP1, which result in notable displacement (shifts) in the calculated phase differences (PLVs). On the other hand, box (c) is selected such that a low-value analytic envelope in four other electrodes

[3] All source codes related to this paper shall be provided online after the publication of the current study.

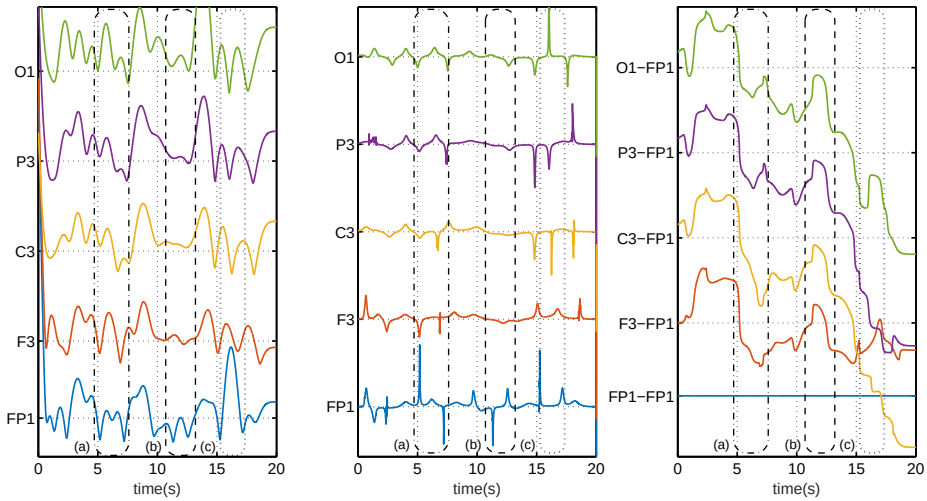

Figure 13: Time domain synchrony (middle panel), the corresponding PLV index (right-side panel), and the instantaneous analytical signal envelope (left-side panel). Notice the estimations affected by low values of analytic envelope .

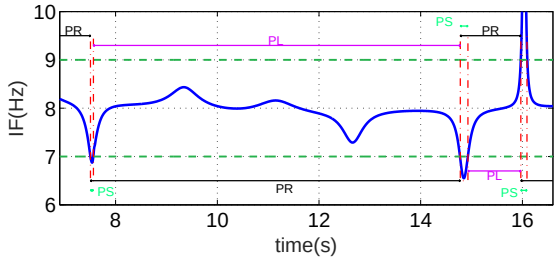

Figure 14: Illustration of Phase Resetting (PR), Phase Lock (PL) and Phase Shift (PS) events using the IF and IP of an EEG segment. The dashed green lines indicate the tunable threshold used for measuring PS [11].

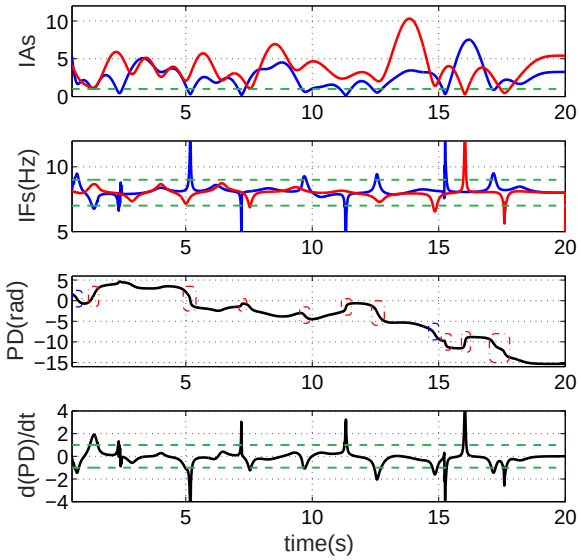

Figure 15: Phase resetting (phase shift) measurements affected by the low values in analytic envelope.

is concurrent with a high envelope in FP1. Again, the phase differences are significantly affected by unreliable spikes in phase sequences due to low IE in these channels. Apparently, as discussed before, measurements of instantaneous phase in time instants with low IE is unreliable and any phase-related quantities such as phase lock, phase difference, or PLV are affected by this issue and any physiological and pathological interpretations based on these quantities require further consideration.

7.2. Phase Resetting

Phase resetting has been defined as a phase shift (PS) followed by a phase difference stability, i.e., phase lock (PL) [16]. Each pair of PS and PL, starting from the beginning of a PS and finishing by the end of a PL (beginning of the next PS), is called a phase reset (PR). Fig. 14 shows the PR, PL and PS events calculated for a typical EEG.

Using the concepts presented in Fig. 14, in Fig. 15 phase shifts are estimated for segments of two EEG channels (FP1 and O1) together with their IE, IF, PD and the first order time difference of the PD. Accordingly, among all the detected phase shift events (curves crossing the green dashed *threshold* in second panel), only two of them have occurred in significantly high IE (may be considered relevant). Furthermore, according to the third and fourth panels, the phase shifts calculated between two channels are only relevant only during the epochs where the IE of both channels have been above the threshold (blue boxes) and the rest of the detected phase shift events (red boxes) are unreliable, due to the low-envelope analytic signal.

Phase resetting in various frequency bands of cerebral signals have been previously correlated to different cognitive responses such as working memory [42, 43], brain development [44], intelligence [45, 46], consciousness [47, 48, 49, 50], sensory-motor interactions [51] and many more [52, 53]. While many

of the phase shifts and resettings have been during unreliable IE magnitudes. This raises some reservations regarding physiological and pathological interpretations which have been based on phase resetting of brain signals and highlights the necessity of simultaneous IE analysis for such applications, either as a complement or replacement for phase analysis.

7.3. Phase-Amplitude Coupling (PAC)

Phase amplitude coupling (PAC) is a means of investigating the coupling between the phase of lower frequency oscillations and the power of higher frequency oscillations, i.e., synchronization of IE of faster rhythms with IP of slower rhythms [54]. Due to the algorithmic details of the PAC, its study is beyond the scope of the current study. However, many aspects of PAC, including the calculation of the IP and IE in different frequency bands can be studied within the hereby proposed scheme. Specifically, the current study emphasizes the necessity of a Monte Carlo estimation of the IE, IP and IF for PAC studies to assure the statistical relevance of the calculated index.

8. Discussion and Conclusion

In this study the classical procedure of instantaneous EEG phase and frequency analysis was studied in a stochastic Monte Carlo estimation framework and justified using the most widely accepted data model representing foreground and background EEG activities. The probability density functions of the instantaneous phase and envelope and their dependence on the instantaneous SNR of the EEG were derived. By using minor perturbations in the BP filtering scheme and background noise level, it was shown that the EEG phase parameters are highly dependent on the IE and are statistically unreliable in low analytical signal envelopes. The impact of this framework was shown for EEG IP and IF calculation, and well-known phase-based parameters such as phase synchrony, PLV and phase resetting. The study raises some major reservations on the interpretation of previously reported physiological factors, which have been derived from the EEG phase alone (neglecting the envelope information). Considering the high impact of the IE on IP and IF, a fundamental question is whether phase related indexes can be considered as independent cerebral factors, or they are merely side effects of the IE variations. The answer to this question requires a statistical setup on a large dataset recorded under well-defined brain experiments such as steady state audio/visual evoked potentials.

In future studies, the hereby proposed Monte Carlo randomization procedure and post-processing proposed in Section 4 can also be unified using *particle filtering* or *sequential Monte Carlo filtering*, which perform randomization and smoothing at the same time and provides sample-based MAP estimates for the EEG phase and frequency.

In case of wide acceptance, the findings of this research can set forth new standards for EEG phase/frequency estimation methods, using multiple and infinitesimal algorithm parameter variations and the necessity of reporting average and confidence intervals over these Monte Carlo sweeps.

Acknowledgment

This research has been supported by the Cognitive Sciences and Technologies Council of Iran (COGC), under the grant number 2250.

References

[1] T. W. Picton, A. Dimitrijevic, M. S. John, P. Van Roon, The use of phase in the detection of auditory steady-state responses, Clinical Neurophysiology 112 (9) (2001) 1698–1711. doi:10.1016/S1388-2457(01)00608-3.

[2] D. J. Krusienski, D. J. McFarland, J. R. Wolpaw, Value of amplitude, phase, and coherence features for a sensorimotor rhythm-based brain–computer interface, Brain research bulletin 87 (1) (2012) 130–134. doi:10.1016/j.brainresbull.2011.09.019.

[3] J. Fell, N. Axmacher, The role of phase synchronization in memory processes, Nature reviews neuroscience 12 (2) (2011) 105–118. doi:10.1038/nrn2979.

[4] M. Siegel, M. R. Warden, E. K. Miller, Phase-dependent neuronal coding of objects in short-term memory, Proceedings of the National Academy of Sciences 106 (50) (2009) 21341–21346. doi:10.1073/pnas.0908193106.

[5] V. Sakkalis, Review of advanced techniques for the estimation of brain connectivity measured with eeg/meg, Computers in biology and medicine 41 (12) (2011) 1110–1117. doi:10.1016/j.compbiomed.2011.06.020.

[6] K. J. Friston, Functional and effective connectivity: a review, Brain connectivity 1 (1) (2011) 13–36. doi:10.1089/brain.2011.0008.

[7] M. Chávez, M. Le Van Quyen, V. Navarro, M. Baulac, J. Martinerie, Spatio-temporal dynamics prior to neocortical seizures: amplitude versus phase couplings, IEEE Transactions on Biomedical Engineering 50 (5) (2003) 571–583. doi:10.1109/TBME.2003.810696.

[8] T. I. Netoff, S. J. Schiff, Decreased neuronal synchronization during experimental seizures, The Journal of neuroscience 22 (16) (2002) 7297–7307.

[9] C. Stam, Y. Van Der Made, Y. Pijnenburg, P. Scheltens, EEG synchronization in mild cognitive impairment and alzheimer's disease, Acta Neurologica Scandinavica 108 (2) (2003) 90–96. doi:10.1034/j.1600-0404.2003.02067.x.

[10] C. J. Stam, A. M. v. C. van Walsum, Y. A. Pijnenburg, H. W. Berendse, J. C. de Munck, P. Scheltens, B. W. van Dijk, Generalized synchronization of MEG recordings in Alzheimers disease: evidence for involvement of the gamma band, Journal of Clinical Neurophysiology 19 (6) (2002) 562–574.

[11] R. W. Thatcher, D. M. North, J. Neubrander, C. J. Biver, S. Cutler, P. DeFina, Autism and EEG phase reset: deficient GABA mediated inhibition in thalamo-cortical circuits, Developmental neuropsychology 34 (6) (2009) 780–800. doi:10.1080/87565640903265178.

[12] B. Blankertz, L. Acqualagna, S. Dähne, S. Haufe, M. Schultze-Kraft, I. Sturm, M. Uščumlic, M. A. Wenzel, G. Curio, K.-R. Müller, The Berlin Brain-Computer Interface: Progress Beyond Communication and Control, Frontiers in Neuroscience 10. doi:10.3389/fnins.2016.00530.

[13] I. Sturm, S. Bach, W. Samek, K.-R. Müller, Interpretable Deep Neural Networks for Single-Trial EEG Classification, arXiv preprint arXiv:1604.08201doi:10.1016/j.jneumeth.2016.10.008.

[14] M. Chavez, M. Besserve, C. Adam, J. Martinerie, Towards a proper estimation of phase synchronization from time series, Journal of neuroscience methods 154 (1) (2006) 149–160. doi:10.1016/j.jneumeth.2005.12.009.

[15] W. J. Freeman, B. C. Burke, M. D. Holmes, Aperiodic phase re-setting in scalp eeg of beta–gamma oscillations by state transitions at alpha–theta rates, Human brain mapping 19 (4) (2003) 248–272.

[16] A. Pikovsky, M. Rosenblum, J. Kurths, Synchronization: a universal concept in nonlinear sciences, Vol. 12, Cambridge university press, 2003.

[17] J. M. Hurtado, L. L. Rubchinsky, K. A. Sigvardt, Statistical method for detection of phase-locking episodes in neural oscillations, Journal of Neurophysiology 91 (4) (2004) 1883–1898. doi:10.1152/jn.00853.2003.

[18] R. L. Freeman WJ, Fine temporal resolution of analytic phase reveals episodic synchronization by state transitions in gamma EEG, Journal of Neurophysiology 87 (2002) 937945. doi:10.1152/jn.00254.2001.

[19] M. Le Van Quyen, J. Foucher, J.-P. Lachaux, E. Rodriguez, A. Lutz, J. Martinerie, F. J. Varela, Comparison of Hilbert transform and wavelet methods for the analysis of neuronal synchrony, Journal of neuroscience methods 111 (2) (2001) 83–98. doi:10.1016/S0165-0270(01)00372-7.

[20] W. A. Rios Herrera, J. Escalona, D. Rivera López, M. F. Müller, On the estimation of phase synchronization, spurious synchronization and filtering, Chaos: An Interdisciplinary Journal of Nonlinear Science 26 (12) (2016) 123106. doi:10.1063/1.4970522.

[21] B. Boashash, Estimating and interpreting the instantaneous frequency of a signal. I. Fundamentals, Proceedings of the IEEE 80 (4) (1992) 520–538.

[22] B. Boashash, Estimating and interpreting the instantaneous frequency of a signal. II. Algorithms and applications, Proceedings of the IEEE 80 (4) (1992) 540–568.

[23] B. Picinbono, On instantaneous amplitude and phase of signals, Signal Processing, IEEE Transactions on 45 (3) (1997) 552–560.

[24] E. Seraj, R. Sameni, Robust electroencephalogram phase estimation with applications in brain-computer interface systems, Physiological Measurement 38 (3) (2017) 501. doi:10.1088/1361-6579/aa5bba.

[25] F. Karimzadeh, E. Seraj, R. Boostani, R. Sameni, A distributed classification procedure for automatic sleep stage scoring based on instantaneous electroencephalogram phase and envelope features, IEEE Transactions on Neural Systems & Rehabilitation Engineering[Manuscript under review].

[26] W. J. Freeman, Hilbert transform for brain waves, Scholarpedia 2 (1) (2007) 1338.

[27] P. Sauseng, W. Klimesch, W. Gruber, S. Hanslmayr, R. Freunberger, M. Doppelmayr, Are event-related potential components generated by phase resetting of brain oscillations? a critical discussion, Neuroscience 146 (4) (2007) 1435–1444. doi:10.1016/j.neuroscience.2007.03.014.

[28] V. Mäkinen, H. Tiitinen, P. May, Auditory event-related responses are generated independently of ongoing brain activity, Neuroimage 24 (4) (2005) 961–968. doi:10.1016/j.neuroimage.2004.10.020.

[29] A. Mazaheri, O. Jensen, Posterior α activity is not phase-reset by visual stimuli, Proceedings of the National Academy of Sciences of the United States of America 103 (8) (2006) 2948–2952. doi:10.1073/pnas.0505785103.

[30] W. B. Davenport, W. L. Root, An introduction to the theory of random signals and noise, Vol. 159, McGraw-Hill New York, 1958.

[31] S. O. Rice, Statistical properties of a sine wave plus random noise, Bell System Technical Journal 27 (1) (1948) 109–157.

[32] H. Raemer, R. Blyth, The probability density of the phase difference of a narrow-band gaussian noise with sinusoidal signal (corresp.), IRE Transactions on Information Theory 7 (4) (1961) 265–267.

[33] Y. S. Shmaliy, Probability distributions of the envelope and phase, and their derivatives in time of the sum of a non-stationary sine signal and narrow-band gaussian noise, Journal of the Franklin Institute 336 (6) (1999) 1013–1022.

[34] S. M. Kay, Fundamentals of Statistical Signal Processing: Estimation Theory, Prentice Hall PTR, 1993.

[35] M. L. Farquharson, Estimating the parameters of polynomial phase signals, Ph.D. thesis, Queensland University of Technology (2006).

[36] S. Peleg, B. Porat, The Cramer-Rao lower bound for signals with constant amplitude and polynomial phase, IEEE Transactions on Signal Processing 39 (3) (1991) 749–752. doi:10.1109/78.80864.

[37] M. A. Richards, Fundamentals of radar signal processing, Tata McGraw-Hill Education, 2005.

[38] R. Sameni, A Linear Kalman Notch Filter for Power-Line Interference Cancellation, in: Proceedings of the 16th CSI International Symposium on Artificial Intelligence and Signal Processing (AISP), Shiraz, Iran, 2012, pp. 604–610.

[39] R. Sameni, The Open-Source Electrophysiological Toolbox (OSET), version 3.1 (2014).
URL http://www.oset.ir

[40] J.-P. Lachaux, E. Rodriguez, J. Martinerie, F. J. Varela, Measuring phase synchrony in brain signals, Human brain mapping 8 (4) (1999) 194–208.

[41] M. G. Rosenblum, A. S. Pikovsky, J. Kurths, Phase synchronization of chaotic oscillators, Physical review letters 76 (11) (1996) 1804. doi:10.1103/PhysRevLett.76.1804.

[42] D. S. Rizzuto, J. R. Madsen, E. B. Bromfield, A. Schultz-Bonhage, R. A.-S. D. Seelig, M. J. Kahana, Reset of human neocortical oscillations during a working memory task, Proc. Natl. Acad. Sci 100 (2003) 7931–7936. doi:10.1073/pnas.0732061100.

[43] C. Tallon-Baudry, O. Bertrand, C. Fischer, Oscillatory synchrony between human extrastriate areas during visual short-term memory maintenance, J Neurosci 21 (20) (2001) 177.

[44] C. B. R. W. Thatcher, D. North, Development of cortical connectivity as measured by EEG coherence and phase, Human Brain Mapping 29 (2008) 1400–1415. doi:10.1002/hbm.20474.

[45] C. B. R.W. Thatcher, D. North, Intelligence and EEG phase reset: A two compartmental model of phase shift and lock, Neuroimage 42 (2008) 1639–1653. doi:10.1016/j.neuroimage.2008.06.009.

[46] P. Sauseng, W. Klimesch, W. R. Gruber, N. Birbaumer, Cross-frequency phase synchronization: A brain mechanism of memory matching and attention, Neuroimage 40 (2008) 308–317. doi:10.1016/j.neuroimage.2007.11.032.

[47] D. Cosmelli, O. David, J. P. Lachaux, J. Martinerie, L. Garnero, B. Renault, F. Varela, Waves of consciousness: ongoing cortical patterns during binocular rivalry, Neuroimage 23 (2004) 128–140. doi:10.1016/S0165-1684(99)00103-6.

[48] F. J. Varela, J. P. Lachaux, E. Rodriguez, J. Martinerie, The brainweb: phase synchronization and large-scale integration, Nature Reviews N 2 (2001) 229–239. doi:10.1038/35067550.

[49] E. R. John, The neurophysics of consciousness, Brain Research Reviews 39 (2002) 1–28. doi:10.1016/S0165-0173(02)00142-X.

[50] E. R. John, From synchronous neural discharges to subjective awareness?, Progress in Brain Research 150 (2005) 143–171. doi:10.1016/S0079-6123(05)50011-6.

[51] E. Vaadia, L. Haalman, M. Abeles, H. Bergman, Y. Prut, H. Slovin, A. Aertsen, Dynamics of neuronal interactions in monkey cortex in relation to behavior events, Nature 373 (1995) 515–518. doi:10.1038/373515a0.

[52] P. Sauseng, W. Klimesch, What does phase information of oscillatory brain activity tell us about cognitive processes?, Neuroscience and Biobehavioral Reviews 32 (2008) 1001–1013. doi:10.1016/j.neubiorev.2008.03.014.

[53] M. J. Kahana, The cogntivie correlates of human brain oscillations, Journal of Neuroscience 26 (2006) 1669–1672. doi:10.1523/JNEUROSCI.3737-05c.2006.

[54] B. Voytek, R. T. Canolty, A. Shestyuk, N. Crone, J. Parvizi, R. T. Knight, Shifts in gamma phase–amplitude coupling frequency from theta to alpha over posterior cortex during visual tasks, Frontiers in human neuroscience 4 (2010) 191.